

Star-Shaped Single-Polymer Systems with Simultaneous RGB Emission: Design, Synthesis, Saturated White Electroluminescence, and Amplified Spontaneous Emission

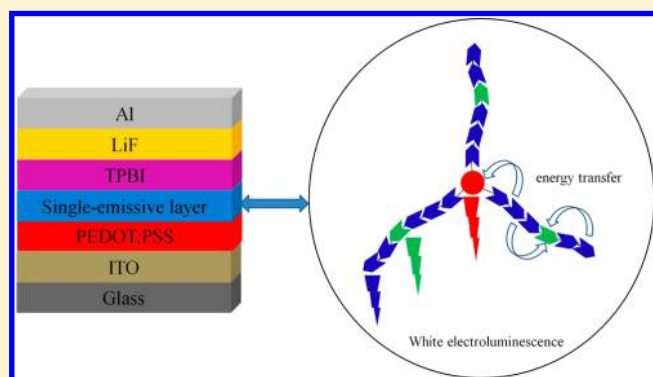
Cheng-Fang Liu,[†] Yuanda Jiu,[†] Jianyun Wang,[†] Jianpeng Yi,[†] Xin-Wen Zhang,[†] Wen-Yong Lai,^{*,†,‡} and Wei Huang^{*,†,‡}

[†]Key Laboratory for Organic Electronics and Information Displays (KLOEID) & Institute of Advanced Materials (IAM), Jiangsu National Synergetic Innovation Center for Advanced Materials (SICAM), Nanjing University of Posts & Telecommunications, 9 Wenyuan Road, Nanjing 210023, China

[‡]Key Laboratory of Flexible Electronics (KLOFE) & Institute of Advanced Materials (IAM), Jiangsu National Synergetic Innovation Center for Advanced Materials (SICAM), Nanjing Tech University (NanjingTech), 30 South Puzhu Road, Nanjing 211816, China

S Supporting Information

ABSTRACT: A three-armed star-shaped single-polymer system comprising tris(4-(3-hexyl-5-(7-(4-hexylthiophen-2-yl)-benzo[*c*][1,2,5]thiadiazol-4-yl)thiophen-2-yl)phenyl)amine (TN) as red emissive cores, benzothiadiazole (BT) as green emissive dopants, and polyfluorene (PF) as blue arms was successfully developed, in which the construction of the star-shaped architectures can depress intermolecular interactions and concentration quenching. The thermal, photophysical, electrochemical, electroluminescent, and amplified spontaneous emission (ASE) properties of the synthesized polymers are systematically investigated. The modulation of the doping concentration of TN and BT can guarantee the partial energy transfer in a star-shaped single-polymer system, further achieving saturated white emission. Consequently, a current efficiency of 2.41 cd A⁻¹ and Commission Internationale d'Éclairage (CIE) coordinates of (0.34, 0.35) were recorded for TN-R3G4 with 0.03 mol % red core and 0.04 mol % green dopants. The saturated white emission is likely to result from the fine control of partial energy transfer and suppressed intermolecular interactions due to the construction of such a star-shaped single-polymer system. What is more, TN-R3G4 shows impressive ASE characteristics with relatively low threshold of 63 ± 5 μJ/cm², which demonstrates the potential as gain media for organic lasing applications. Our results have provided new insights and better understanding into the photophysical and optoelectronic behaviors of the resulting star-shaped single-polymer systems with simultaneous RGB emission.



INTRODUCTION

During the past decade, white polymer light-emitting diodes (WPLEDs) have gained remarkable attention because of their various applications in full-color displays and solid-state lighting.^{1–5} The most widely employed methods for fabricating WPLEDs have been reported, which involve the multilayer system with sequential deposition of red, green, and blue (RGB) emissive species⁶ and physical blends such as polymer–small molecule blend systems,^{7,8} polymer–organometallic complex blend systems,⁹ and polymer–polymer blend systems.^{10,11} The multilayer device may encounter the mixing of adjacent layers, which is detrimental to the device performance. In contrast, the blended devices have undergone significant development in efficiency and brightness. However, the phase behavior is sensitive to the driving voltages and operational conditions, thus resulting in unstable electroluminescence (EL) spectra and color coordinates.

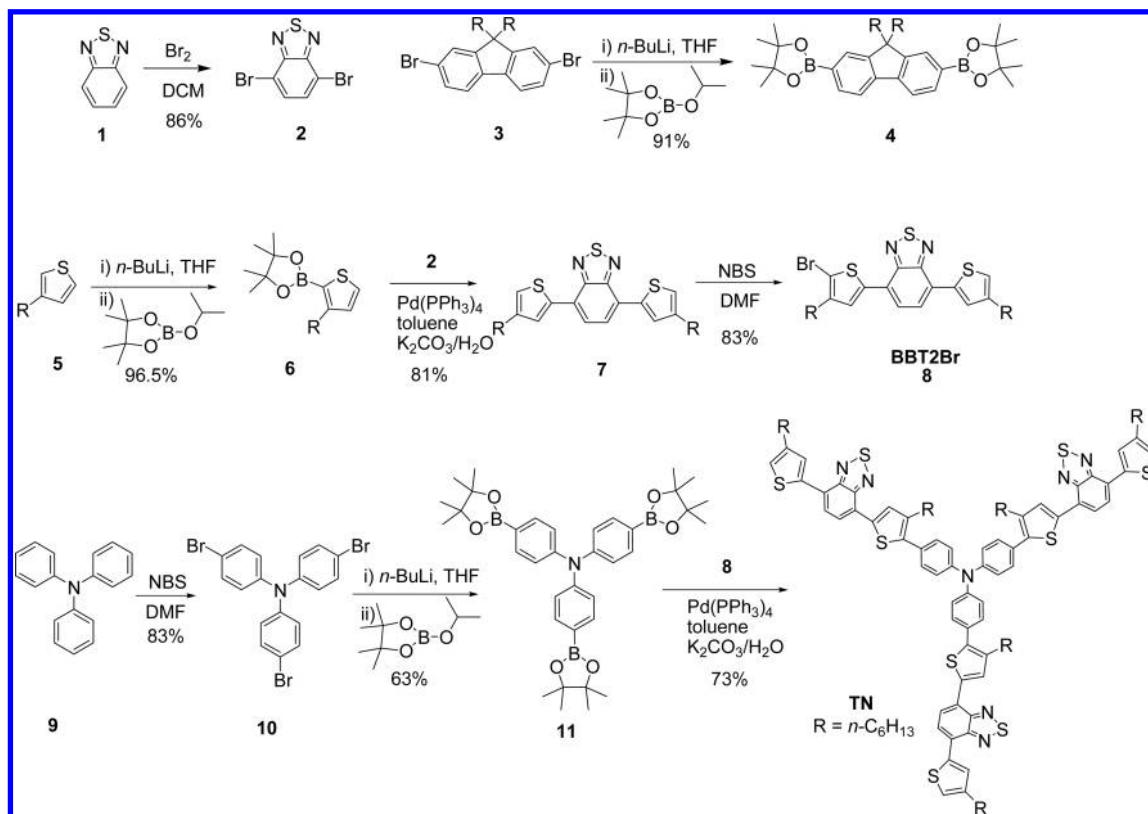
To address these issues, great efforts have been made to a single-polymer system^{12–16} based on the insufficient energy transfer because phase separation of chromophores can be largely suppressed by incorporating RGB emissive species into a single-polymer chain. Recently, many groups have concentrated on linear single-polymer systems to accomplish white emission, in which the energy transfer can be fine-tuned by modulating the contents of various emissive components, further manifesting comparably stable bias-independent EL spectra. Wang and co-workers¹² developed a novel method in which a green-emitting component was attached to the pendant chain and a red-emitting component was incorporated into the blue-emitting polyfluorene backbone, realizing white emission with maximum current

Received: January 4, 2016

Revised: March 6, 2016

Published: March 22, 2016

Scheme 1. Synthetic Routes toward the Core Structure TN



efficiency of 1.59 cd A^{-1} and CIE coordinates of (0.31, 0.34). Lee et al.¹³ developed a copolymer comprising 9,9-dihexylfluorene as blue emissive species and 2-(2,6-bis{2-[1-(9,9-dihexyl-9H-fluoren-2-yl)-1,2,3,4-tetrahydroquinolin-6-yl]vinyl}pyran-4-ylidene)malononitrile (DCMF) as orange emissive species. The electroluminescent devices showed maximum current efficiency of 0.60 cd A^{-1} and CIE coordinates of (0.33, 0.31). Generally speaking, linear single-polymer systems have suppressed phase separation and bias-independent EL performance but encounter low efficiency and unsaturated white emission in comparison to the blend systems. Therefore, it is imperative to develop novel white-light-emitting single-polymer materials with improved efficiency and saturated emission.

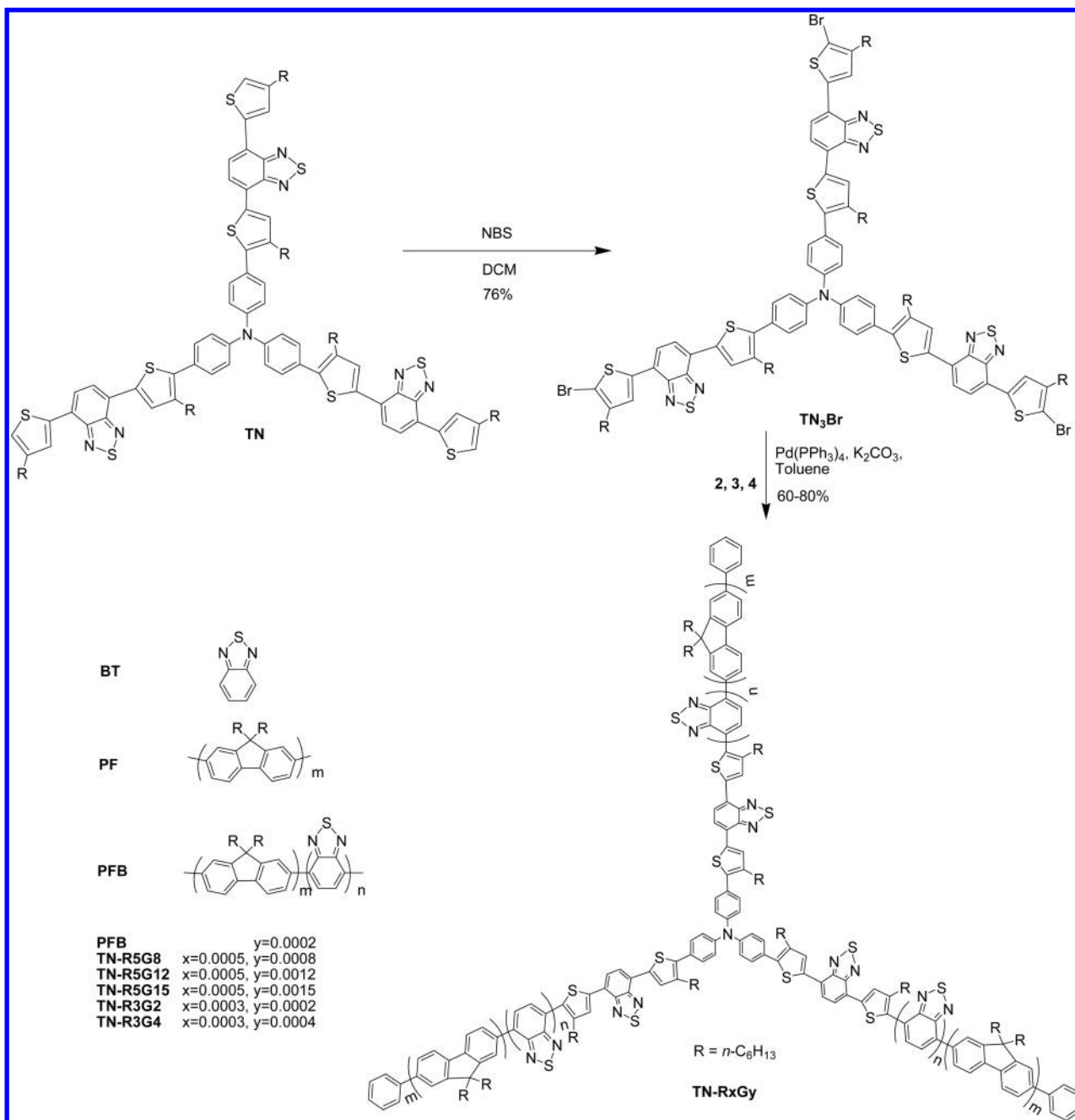
According to previous studies in our group, monodisperse conjugated star-shaped macromolecules have been developed with high purity, well-defined chemical structures, good solution processability, and excellent optoelectronic characteristics.^{17–23} It is notable to mention that PLEDs based on these macromolecules exhibited highly efficient blue and red emission. Thus, making use of the star-shaped architectures, we can incorporate various emissive components to ensure the insufficient energy transfer, further realizing white emission. Star-shaped polymer systems have attracted much interest owing to the highly branched architectures, suppressed intermolecular interactions, and improved solid-state luminescence.^{24–29} Hyperbranched copolymers with phenylene units as the blue host and benzothiadiazole derivatives as red and green chromophores were developed by Kim's group,³⁰ demonstrating white EL with CIE coordinates of (0.32, 0.35). WPLEDs based on these copolymers exhibited a maximum luminous efficiency (LE) of 0.21 cd A^{-1} , which still need further optimization to satisfy the requirements of commercial applications. The

investigation on the novel materials with saturated and stable white emission is still going on.

In this article, we reported white EL from a star-shaped single-polymer system synthesized by introducing polyfluorene (PF) as blue emissive arms and 2,1,3-benzothiadiazole (BT) as green emissive dopants onto tris(4-(3-hexyl-5-(7-(4-hexylthiophen-2-yl)benzo[*c*][1,2,5]thiadiazol-4-yl)thiophen-2-yl)phenyl)amine (TN) as the red emissive core. Here, TN was selected as the core because of its saturated red emission. Blue PF arms were used in the system due to their high photoluminescence efficiency and good thermal and electrochemical stability. BT units were widely applied in the design of novel materials for green light emission. The synthesis, thermal stability, photophysical, electrochemical, and electroluminescent characteristics and amplified spontaneous emission (ASE) properties of these resulting polymers were studied in detail. By modulating the content of TN and BT, we controlled the insufficient energy transfer from the blue arms to the green and red species, therefore achieving saturated white emission with simultaneous blue (442 nm), green (495 nm), and red (625/608 nm) emission. A single-emissive-layer device based on the polymer (TN-R3G4) achieved high-color-quality white EL with a current efficiency of 2.41 cd A^{-1} and CIE coordinates of (0.34, 0.35). Interestingly, typical ASE behaviors could also be detectable from the resulting star-shaped single-polymer system with low content of red and green emissive dopants in films. A relatively low threshold of $63 \pm 5 \mu\text{J}/\text{cm}^2$ with ASE peaks at 448 nm was recorded for TN-R3G4, showing great promise for organic lasing applications.

RESULTS AND DISCUSSION

The synthetic routes toward the model compounds and the resulting polymers are shown in Schemes 1 and 2. A₃(arm-three)-type core structure was obtained from bromination of the

Scheme 2. Schematic Illustrations and Synthetic Routes of TN-R_xG_y^a

^a*x* means the contents of TN as red dopants, and *y* denotes the contents of BT as green dopants.

star-shaped red emissive molecule (TN) with *N*-bromosuccinimide (NBS). According to Suzuki polycondensation, star-shaped polymers were synthesized from an AB type 9,9-dioctylfluorene monomer, a green 2,1,3-benzothiadiazole monomer, and an A₃-type red emissive core. The polymers are named as TN-R_{*x*}G_{*y*}, where *x* means the contents of TN as red dopants and *y* denotes the contents of BT as green dopants. The doping concentration of TN and BT was controlled to tune the relative intensity of the blue, green, and red emission. For TN-R5G8, TN-R5G12, and TN-R5G15, the content of the red unit was fixed at 0.05 mol % while the content of the green dopants was controlled as 0.08, 0.12, and 0.15 mol % (Table S1), respectively. The similar adjustment in doping concentration was applied for TN-R3G2 and TN-R3G4. By comparison, we also

synthesized polyfluorene homopolymer (PF) and poly(9,9-dihexylfluorene-*co*-benzothiadiazole) (PFB) as model compounds.

As revealed by thermogravimetric analysis (TGA) and differential scanning calorimetry (DSC) measurements in Figure S1a,b, TN has the decomposition temperature (*T_d*, corresponding to 5% weight loss) of 402 °C. The glass transition temperature (*T_g*) was noticed at 157 °C. Moreover, the resulting polymers exhibited excellent thermal stability as shown in Figure S2. In order to unravel the packing structures in condensed states of the polymers, wide-angle X-ray diffraction (WXR) measurements were implemented. The results confirmed that all the polymers possessed typical amorphous characteristics (Figure S3).

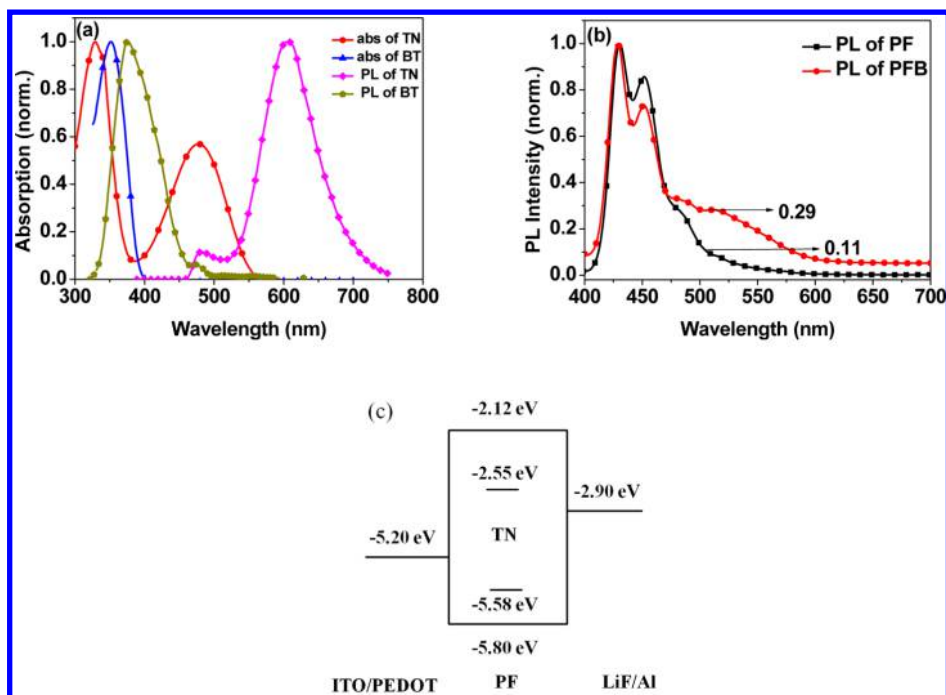


Figure 1. (a) Absorption spectra and PL spectra of TN and BT in dilute solutions. (b) PL spectra of PF and PFB in solid films. (c) Energy levels of TN and PF.

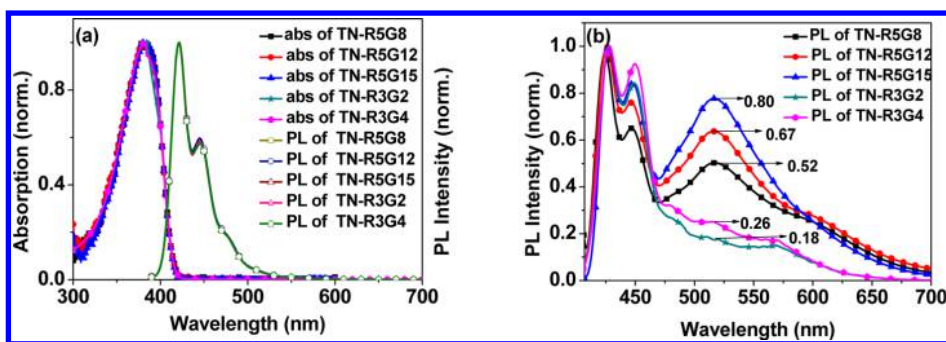


Figure 2. (a) UV-vis absorption and PL spectra of the star-shaped polymers in THF solutions. (b) PL spectra of the star-shaped polymers in solid films.

Figure 1a shows the absorption and photoluminescence (PL) spectra of TN and BT in dilute solutions. Two well-resolved absorption bands at 329 and 477 nm are observed for TN. BT shows absorption peak at 351 nm and the PL emission peak at 480 nm. Figure 1b shows PL spectra of PF and PFB in solid films. The absorption spectra of all the polymers in Figure 2a show peaks at around 384 nm, which are attributed to the π - π^* transition of PF backbones. Since the doping concentration is extremely low, the absorption of red dopants at 475/457 nm and green dopants at 353 nm can be hardly detected. In dilute solutions, these polymers have similar PL spectra to PF because of the fluorene segment. Nevertheless, the polymers in the films show PL spectra with red emission from TN core, green emission from BT dopants, and blue emission from PF arms (Figure 2b). The doping concentration of the red and green dopants were adjusted to generate partial energy transfer, thus achieving white EL. It is indicated that the different contents of the red TN core and green BT units significantly affect the PL spectra. Increasing the doping concentration resulted in obvious enhancement of the relative intensity of the red and green emission. For instance, TN-R5G15 has the highest intensity of the green emission in this system, originating from the high contents of BT green dopants.

Under this circumstance, the energy transfer has become complete in the process, which is disadvantageous to generate white emission. In contrast, TN-R3G4 exhibits the balance of RGB emission with optimized contents in such a star-shaped single-polymer system.

Figure 1c shows the lowest unoccupied molecular orbital (LUMO) and highest occupied molecular orbital (HOMO) energy levels of TN and PF. Both of HOMO and LUMO energy levels of TN are situated between the HOMO/LUMO energy levels of PF, implying efficient charge trapping in EL process. The electrochemical properties of polymers are shown in Figure S4 and summarized in Table S3. The results suggest that the energy levels could be barely affected by the doping concentration because of the extremely low contents.

To study the EL properties of the resulting polymers, single-emissive-layer devices with configuration of indium-tin oxide (ITO)/poly(3,4-ethylenedioxythiophene):poly(styrene-sulfonate) (PEDOT:PSS) (40 nm)/polymer (80 nm)/1,3,5-tris(1-phenyl-1H-benzimidazol-2-yl)benzene (TPBI) (30 nm)/LiF (1 nm)/Al (80 nm) were fabricated. The devices were thermally annealed at 120 °C for 10 min in a vacuum box before the LiF/Al cathode was evaporated. As shown in Figure 3a, the

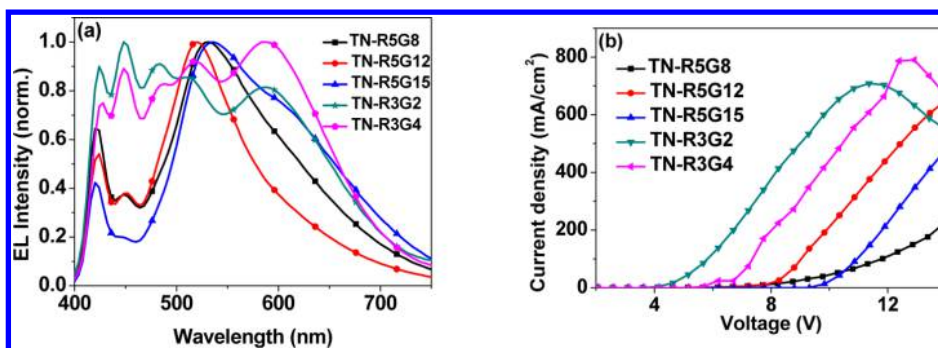


Figure 3. (a) EL spectra and (b) voltage–current density of the devices based on TN-RxGy.

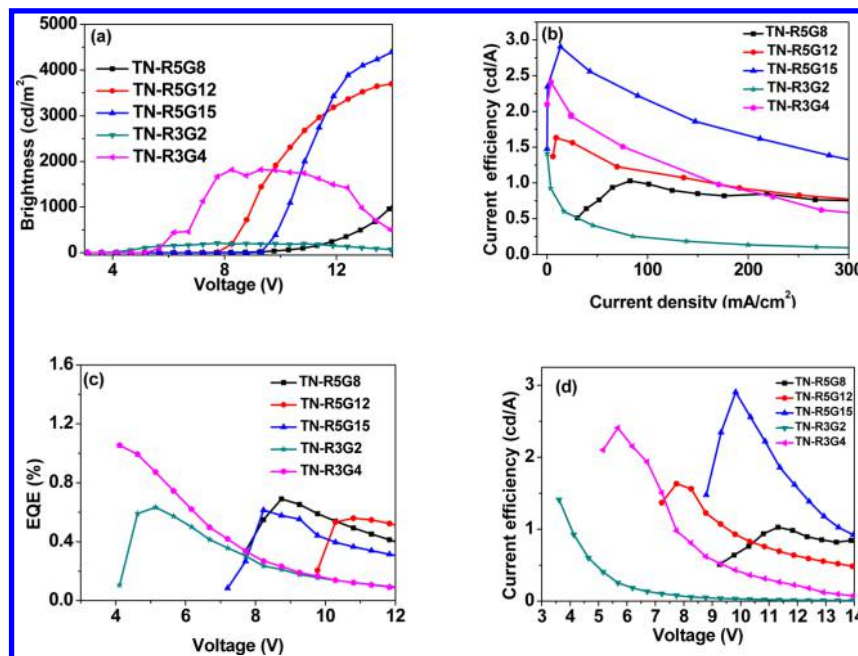


Figure 4. EL characteristics of TN-RxGy with the configuration of ITO/PEDOT:PSS/polymer/TPBI/LiF/Al: (a) brightness–voltage characteristics; (b) current efficiency–current density characteristics; (c) EQE–voltage characteristics; (d) current efficiency–voltage characteristics.

Table 1. EL Performance of the Devices

	turn-on voltage [V]	current efficiency [cd A^{-1}]	power efficiency [lm W^{-1}]	maximum brightness [cd m^{-2}]	EQE [%]	GPC		
						M_n	PDI	CIE (x, y)
TN-R5G8	8	1.04	0.29	3041	0.69	9248	1.54	(0.31, 0.40)
TN-R5G12	8	1.64	0.66	3712	0.56	9436	1.88	(0.28, 0.42)
TN-R5G15	8	2.90	0.93	4546	0.61	9430	1.97	(0.30, 0.36)
TN-R3G2	4	1.41	1.24	400	0.63	10990	1.79	(0.33, 0.35)
TN-R3G4	5	2.41	1.33	1833	1.05	11256	1.83	(0.34, 0.35)
TN-blended	5	0.71	0.27	1250	0.25			(0.31, 0.47)

blue, green, and red emission of the EL spectra can be assigned as an individual emission from PF, BT, and TN, respectively. The relative intensity of the peaks in the EL spectra of TN-RxGy can be fine-tuned by varying the contents of the dopants. For TN-R3G2 and TN-R3G4 with the same doping concentration of red core, the relative intensity of the green emission band in the EL spectra increases by increasing the content of green dopants, which is attributed to more energy transfer from the blue arms to the green dopants. A similar phenomenon can also be observed for the case of TN-R5G8, TN-R5G12, and TN-R5G15. Therefore, adjusting the doping concentration is an effective methodology to generate partial energy transfer with the aim to

realize high-quality white emission in such a star-shaped single-polymer system. According to the EL spectra, the CIE coordinates of (0.34, 0.35) were recorded from TN-R3G4, which are very close to the values of standard white emission (0.33, 0.33). More importantly, the EL spectra of TN-R3G4 are quite stable with variation in CIE coordinates of (± 0.02 , ± 0.02) by increasing the bias from 6 to 13 V. Voltage–current density characteristics of the devices are shown in Figure 3b.

Figure 4 shows the brightness–voltage, current efficiency–current density, EQE–voltage, and current efficiency–voltage curves of the devices of TN-RxGy. The detailed data of the corresponding devices are summarized in Table 1. In this system,

current efficiency and maximum brightness are enhanced by increasing the doping concentration, manifesting the suppressed concentration quenching in the doping concentration range. Among these, the device based on TN-R3G4 showed much better white emission with a turn-on voltage of 5.0 V, a maximum brightness of 1833 cd m⁻², a maximum current efficiency of 2.41 cd A⁻¹, and a power efficiency of 1.33 lm W⁻¹.

As a comparison experiment, we have physically blended 0.03 mol % TN into PFB and fabricated a device with the blend as the emissive layer. As shown in Table 1 and Figure S5, the EL spectra exhibited bias dependence. The CIE coordinates of TN-blended samples change from (0.24, 0.31) to (0.31, 0.47) by increasing the bias from 6 to 13 V. In addition, the devices based on TN-blended samples showed a current efficiency of 0.71 cd A⁻¹ and a maximum EQE of 0.25%. The performance is much worse than those based on the star-shaped single-polymer systems (TN-R3G4). We can deduce from the results that phase separation and concentration quenching could be significantly suppressed in such a star-shaped single-polymer system in comparison to the blend system, giving rise to the improved EL performance.

To investigate the excited state relaxation processes of the synthesized polymers, the fluorescence transients of TN-RxGy in dilute solutions and in films were recorded as plotted in Figure 5.

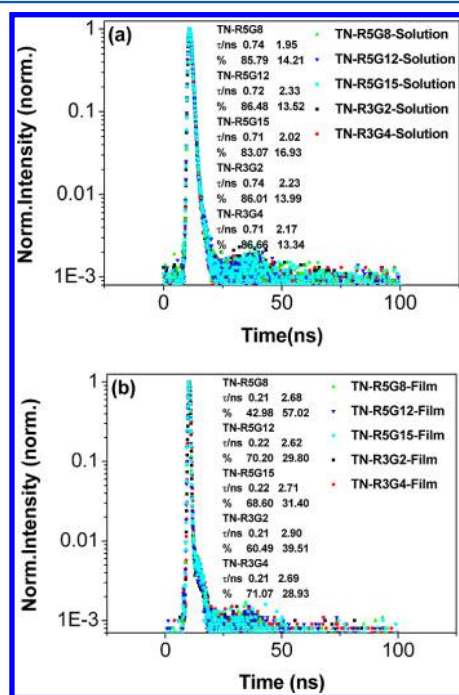


Figure 5. Fluorescence transients of (a) THF solution (10⁻⁵ M) and (b) the films of TN-RxGy measured at the fluorescence band maxima collected at 421 and 447 nm, respectively.

The corresponding transient lifetimes are calculated as listed in the inset. Based on the analysis, the excited state relaxation of TN-RxGy in dilute solutions can be approximated using double-exponential decay profiles, exhibiting a fast component at τ_1 (TN-R5G8) = 0.74 ns (85.79%), τ_1 (TN-R5G12) = 0.72 ns (86.48%), τ_1 (TN-R5G15) = 0.71 ns (83.07%), τ_1 (TN-R3G2) = 0.74 ns (86.01%), τ_1 (TN-R3G4) = 0.71 ns (86.66%) and a longer component at τ_2 (TN-R5G8) = 1.95 ns (14.21%), τ_2 (TN-R5G12) = 2.33 ns (13.52%), τ_2 (TN-R5G15) = 2.02 ns (16.93%), τ_2 (TN-R3G2) = 2.23 ns (13.99%), τ_2 (TN-R3G4) = 2.17 ns (13.34%). The shorter τ_1 for all the polymers are quite similar

and dominated the relaxation decay. It thus should be associated with dominant blue emissive species. The prolonged τ_2 may be attributed to the exciton migration from the blue emissive species to the green or red emissive dopants. It is worthwhile to mention that the resulting star-shaped single-polymer system exhibited quite similar decay patterns in dilute solutions, suggesting little impact of such a rather low content of green and red dopants on the photophysical characteristics.

In addition, the fluorescence transients of the films of TN-RxGy could also be well described by employing a double-exponential decay model with two decay components. The various decay lifetimes in the inset are related with different radiative transition in the system. The shorter τ is about 3 times as short as that observed for solution, while the extracted longer τ is slightly longer than that in solution. To be specific, the shorter τ correlates with the rapid excited state relaxation in an early stage due to the possible more efficient exciton radiation in films. Keeping in mind the molecular aggregation in films, the longer τ varying from about 2 ns can be ascribed to the aggregated states.

High-efficiency and thermally stable conjugated light-emitting polymers have stood out as prominent active materials for organic solid-state lasing.^{19,20,31–34} To get further insights into the photophysical properties of the resulting star-shaped single-polymer systems, the amplified spontaneous emission (ASE) characteristics of TN-RxGy have been investigated consequently. In order to quantify our results, the pulse energy of exciting light at which the full width at half-maximum (fwhm) intensity of the emission spectrum drops to half of its PL value was defined as the ASE threshold.³⁵ As shown in Figures 6a and 6b, since the spectral narrowing emerges only with very high pump energy up to 3338 $\mu\text{J}/\text{cm}^2$, it is indicated that no ASE characteristics are observed for TN-R5G8. In the case of TN-R5G12, the fwhm has dropped dramatically from 27 to 4 nm when pumped above a threshold intensity of $264 \pm 10 \mu\text{J}/\text{cm}^2$. As shown in Figure 6c, the output emission is amplified when the energy of pumped laser pulse is above the threshold. TN-R5G15 has the same ASE characteristics as TN-R5G12 with a threshold intensity of $164 \pm 10 \mu\text{J}/\text{cm}^2$ and the ASE peak at 448 nm (Figure 6e). Meanwhile, as depicted in Figures 6g and 6i, TN-R3G2 and TN-R3G4 have the threshold of 114 ± 10 and $63 \pm 5 \mu\text{J}/\text{cm}^2$ with the ASE peaks at 448 and 448 nm, respectively. In addition, Figures 6b, 6d, 6f, 6h, and 6j show the emission spectra for the planar waveguide of TN-R5G8, TN-R5G12, TN-R5G15, TN-R3G2, and TN-R3G4 with various pump fluences, and the corresponding normalized spectra are depicted in the inset, demonstrating the spectral narrowing. According to the results, the doping concentration plays an important role in ASE characteristics of TN-RxGy. The absence of ASE in TN-R5G8 needs further exploring, and detailed investigation is desirable to clarify the possible reason in this system. Among all these materials, TN-R3G4 with saturated white emission has displayed the lowest threshold of $63 \pm 5 \mu\text{J}/\text{cm}^2$, which is comparable to that of PF ($50 \pm 5 \mu\text{J}/\text{cm}^2$, Figure S6). The results indicated that TN-R3G4 holds great potential as attractive gain media for organic lasing applications. More importantly, this star-shaped single-polymer system was deemed as an attractive platform to investigate the influence of various emissive species with different contents on the energy transfer, in which ASE behaviors could be fine-tuned by adjusting the corresponding concentrations.

CONCLUSIONS

In conclusion, a three-armed star-shaped single-polymer system consisting of TN as red emissive cores, PF as blue emissive arms,

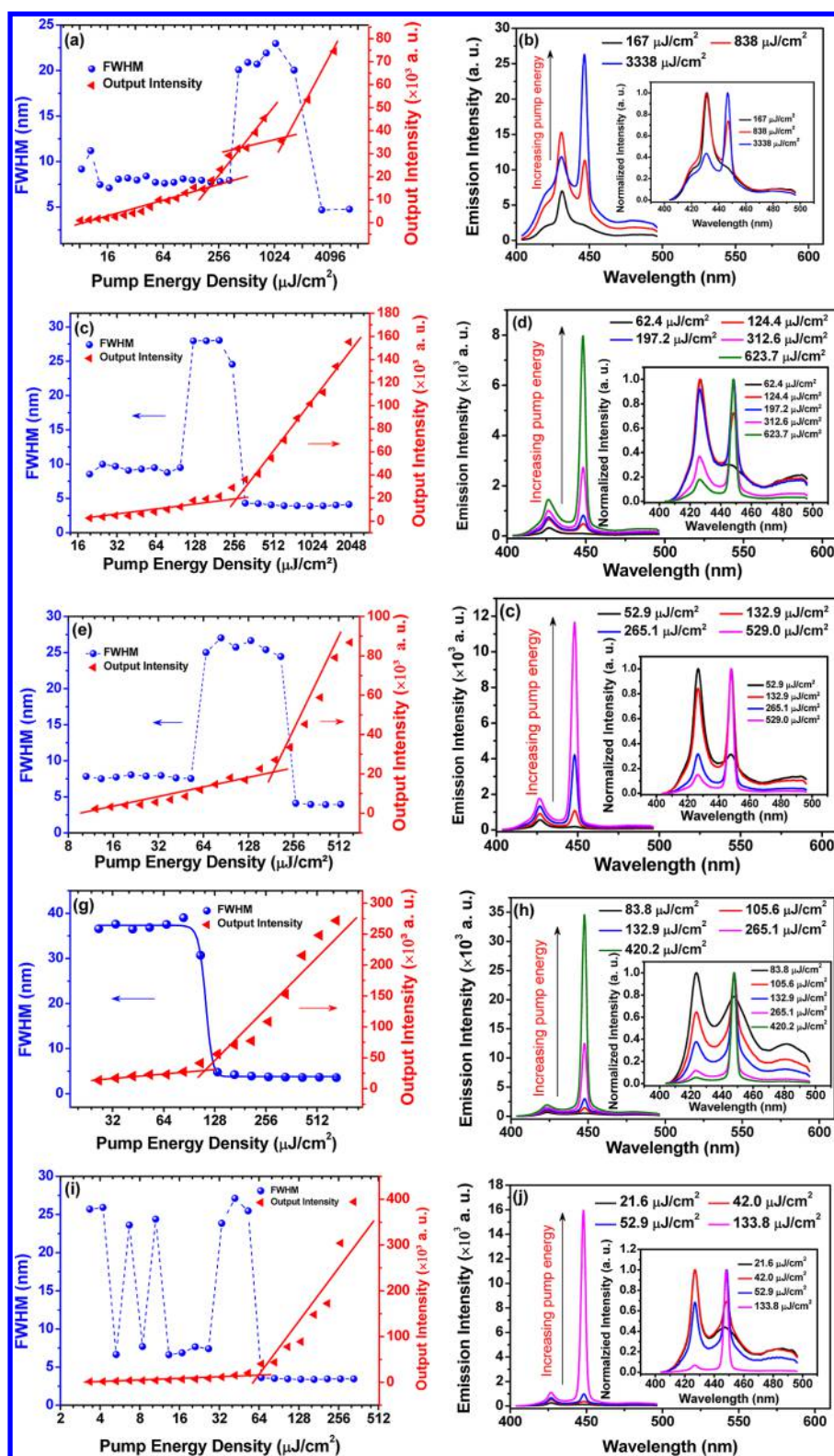


Figure 6. Full width at half-maximum (fwhm) of the emission spectrum (left, solid spheres) and the corresponding output intensity (right, solid triangles) for (a) TN-R5G8, (c) TN-R5G12, (e) TN-R5G15, (g) TN-R3G2, and (i) TN-R3G4 as a function of the pump energy density, indicating its pump threshold. The emission spectra for the planar waveguide of (b) TN-R5G8, (d) TN-R5G12, (f) TN-R5G15, (h) TN-R3G2, and (j) TN-R3G4 with various pump fluences and the corresponding normalized spectra shown in the inset.

and BT as green emissive units was designed and synthesized. According to PL and EL studies, partial energy transfer has played a critical role in achieving good-quality white emission from three primary emissive species. As a result, an appropriate

choice of the doping concentration of TN and BT can facilitate partial energy transfer from the blue components to the red and green dopants, realizing saturated white EL with good CIE coordinates. A current efficiency of 2.41 cd A^{-1} and CIE

coordinates of (0.34, 0.35) were obtained for a single-emissive-layer device based on TN-R3G4. It is notable to mention that their CIE coordinates match well with the values of standard saturated white emission (0.33, 0.33). Keeping all the results in mind, we believe that the star-shaped single-polymer systems appear quite promising to realize high-performance WPLEDs, originating from the fine control of incomplete energy transfer and the suppression of intermolecular interactions and phase separation. Interestingly, the resulting star-shaped single-polymer system with low content of red and green emissive dopants demonstrated typical ASE behaviors. A relatively low threshold of $63 \pm 5 \mu\text{J}/\text{cm}^2$ with ASE peaks at 448 nm was recorded for TN-R3G4, showing great promise for organic lasing applications. Our results have provided new insights and better understanding into the photophysical and optoelectronic behaviors of the resulting star-shaped single-polymer systems with simultaneous RGB emission.

EXPERIMENTAL SECTION

^1H NMR spectra were recorded on a 400 MHz spectrometer. Chloroform (δ 7.26) was used as an internal standard for chloroform-*d*. Fluorescent spectra were recorded on a Shimadzu-S301PC fluorescent spectrometer. UV-vis spectra were recorded on a Shimadzu-3600 spectrometer. Compounds **2**, **4**, **7**, **8**, and **11** were synthesized according to the literature, and the methods for the determination of association constants were reported in our previous papers.^{17–23} TN was synthesized from the Suzuki method.

Synthesis of tris(4-(5-(7-(5-bromo-4-hexylthiophen-2-yl)benzo[*c*]-[1,2,5]thiadiazol-4-yl)-3-hexylthiophen-2-yl)phenyl)amine (TN3Br): A mixture of TN (0.50 g, 0.30 mmol) was dissolved in CH_2Cl_2 (100 mL). Then, NBS (0.16 g, 0.96 mmol) in DMF (5 mL) was added dropwise. Upon complete, the mixture was stirred for an additional 3 h in dark before it was diluted with CH_2Cl_2 , washed with 10% aqueous HCl solution and saturated aqueous NaCl solution, dried (Na_2SO_4), and evaporated. The resulting residue was purified by silica gel column chromatography using hexane/ CH_2Cl_2 (8:1) as eluent to give TN3Br as a dark red solid (0.42 g, 76%). ^1H NMR (400 MHz, CDCl_3), δ (ppm): 8.10 (s, 3H), 7.69–7.77 (m, 9H), 7.46–7.48 (d, 2H), 7.25 (s, 6H), 2.76–2.80 (t, 6H), 2.61–2.65 (t, 6H), 1.64–1.78 (m, 12H), 1.33–1.42 (m, 36H), 0.89–0.91 (t, 18H). ^{13}C NMR (100 MHz, CDCl_3), δ (ppm): 152.47, 152.35, 146.60, 143.00, 139.61, 139.52, 138.73, 136.70, 130.57, 130.08, 129.25, 127.83, 126.06, 124.96, 124.89, 124.77, 124.19, 111.31, 31.93, 31.66, 29.70, 29.36, 22.69, 14.10. Anal. Calcd for $\text{C}_{99}\text{H}_{102}\text{Br}_3\text{N}_7\text{S}_9$: C 61.26, H 5.46, N 5.21, S 15.33. Found: C 61.20, H 5.66, N 5.46, S 15.11.

General Procedures for the Synthesis of the Polymers. To a mixture of 2,7-dibromo-9,9-dihexyl-9H-fluorene (**3**) (quantities given below), 2,2'-(9,9-dihexyl-9H-fluorene-2,7-diyl)bis(4,4,5,5-tetramethyl-1,3,2-dioxaborolane) (**4**), and $\text{Pd}(\text{PPh}_3)_4$ (11.5 mg, 0.01 mmol) under N_2 was added a drop of Aliquat 336, 2 M aqueous potassium carbonate (2.5 mL), and degassed toluene (5 mL). Solutions of tris(4-(5-(7-(5-bromo-4-hexylthiophen-2-yl)benzo[*c*]-[1,2,5]thiadiazol-4-yl)-3-hexylthiophen-2-yl)phenyl)amine (TN3Br) and solutions of 4,7-dibromobenzo[*c*]-[1,2,5]thiadiazole (BT2Br) were also added. The mixture was stirred at 90 °C for 48 h and then poured into methanol. The precipitate was collected by using filtration, dried, and then dissolved in dichloromethane. The solution was washed with water and dried over anhydrous Na_2SO_4 . After most of the solvent had been removed, the residue was poured into stirred methanol to give a fiber-like solid. The polymer was further purified by extracting with acetone for 24 h. The reprecipitation procedure in THF/methanol was then repeated several times. The final product, a light orange-colored fiber, was obtained after drying in a vacuum with a yield of 60–80%. THF was used as the eluent solvent for the GPC measurements.

PF. **3** (0.25 g, 0.50 mmol) and **4** (0.30 g, 0.50 mmol) were used in the polymerization. Gel-permeation chromatography (GPC): $M_n = 2.47 \times 10^4$, polydispersity index (PDI) = 2.09 (polystyrene as standard).

PF. **3** (0.25 g, 0.50 mmol), **4** (0.30 g, 0.50 mmol), and BT2Br (0.2 mL, 1.0×10^{-3} M solution in toluene, 2.0×10^{-4} mmol) were used in the polymerization. GPC: $M_n = 1.19 \times 10^4$, PDI = 1.96 (polystyrene as standard).

TN-R5G8. **3** (0.25 g, 0.50 mmol), **4** (0.30 g, 0.50 mmol), BT2Br (0.8 mL, 1.0×10^{-3} M solution in toluene, 8.0×10^{-4} mmol), and TN3Br (2.5 mL, 2×10^{-4} M solution in toluene, 5.0×10^{-4} mmol) were used in the polymerization. GPC: $M_n = 9248$, PDI = 1.54.

TN-R5G12. **3** (0.25 g, 0.50 mmol), **4** (0.30 g, 0.50 mmol), BT2Br (1.2 mL, 1.0×10^{-3} M solution in toluene, 12.0×10^{-4} mmol), and TN3Br (2.5 mL, 2×10^{-4} M solution in toluene, 5.0×10^{-4} mmol) were used in the polymerization. GPC: $M_n = 9436$, PDI = 1.88.

TN-R5G15. **3** (0.25 g, 0.50 mmol), **4** (0.30 g, 0.50 mmol), BT2Br (1.5 mL, 1.0×10^{-3} M solution in toluene, 15.0×10^{-4} mmol), and TN3Br (2.5 mL, 2×10^{-4} M solution in toluene, 5.0×10^{-4} mmol) were used in the polymerization. GPC: $M_n = 9430$, PDI = 1.97.

TN-R3G2. **3** (0.25 g, 0.50 mmol), **4** (0.30 g, 0.50 mmol), BT2Br (0.2 mL, 1.0×10^{-3} M solution in toluene, 2.0×10^{-4} mmol), and TN3Br (1.5 mL, 2×10^{-4} M solution in toluene, 3.0×10^{-4} mmol) were used in the polymerization. GPC: $M_n = 1.10 \times 10^4$, PDI = 1.79.

TN-R3G4. **3** (0.25 g, 0.50 mmol), **4** (0.30 g, 0.50 mmol), BT2Br (0.4 mL, 1.0×10^{-3} M solution in toluene, 4.0×10^{-4} mmol), and TN3Br (1.5 mL, 2×10^{-4} M solution in toluene, 3.0×10^{-4} mmol) were used in the polymerization. GPC: $M_n = 1.13 \times 10^4$, PDI = 1.83.

All these polymers showed similar ^1H NMR spectra and elemental analysis results. For example, PF: ^1H NMR (400 MHz, CDCl_3) δ (parts per million; ppm): 7.87 (d, 2H), 7.72 (br, 4H), 2.10 (br, 4H), 1.14 (br, 24H), 0.81 (t, 6H). Analysis calculated: C 89.69, H 10.31. Found: C 89.08, H 10.02. The contents of green- and red-light-emitting dopant units in these polymers were too low to be detected using ^1H NMR and elemental analysis.

Device Fabrication and Characterization. OLEDs were fabricated on prepatterned indium–tin oxide (ITO) with the sheet resistance of 10–20 Ω/sq . The substrate was ultrasonic cleaned with acetone, detergent, deionized water, and 2-propanol. Before the film coating, the substrate was treated by oxygen plasma treatment for 4 min. The poly(ethylenedioxythiophene)–poly(styrenesulfonic acid) (PEDOT:PSS) film with thickness of about 40 nm was spin-coated onto the ITO glass. PEDOT:PSS film was dried at 80 °C for 3 h in the vacuum oven. The solution of TN-RxGy polymers in chloroform was prepared under a nitrogen atmosphere and spin-coated onto the PEDOT:PSS layer, resulting in the emitting layer with an approximate thickness of 80 nm. Soon afterward, a thin layer of TPBI (30 nm) as an electron injection cathode and the subsequent LiF (1 nm)/aluminum (80 nm) layers were thermally deposited by vacuum evaporation through a mask at a base pressure below 2×10^{-4} Pa. The luminance of the device was measured with a calibrated photodiode. External quantum efficiency was measured by the integrating sphere. Luminance was calibrated after the encapsulation of devices with UV-curing epoxy and thin cover glasses. The Commission Internationale d'Éclairage (CIE) coordinates were calculated using 1931 observer parameters.

As for ASE characterization, all samples were optically pumped at 355 nm by using an optical parametric oscillator (OPO), which was pumped by a frequency-tripled pulsed Q-switched Nd^{3+} :YAG laser system with 5 ns-output pulses at a repetition rate of 10 Hz. The raw pulsed beam from the OPO passed through an adjustable slit to be spatially formed and then was focused with a cylindrical lens (with focal length $f = 10$ cm) to form a 4.1 mm \times 440 μm stripe-shaped excitation area on the sample. The pump energy incident on the sample was tuned by the insertion of a set of calibrated neutral density filters into the beam path. The emission was collected from the edge of the slab waveguide by a fiber-coupled spectrograph and recorded by a charge coupled device (CCD) detector.

ASSOCIATED CONTENT

Supporting Information

The Supporting Information is available free of charge on the ACS Publications website at DOI: 10.1021/acs.macromol.6b00020.

TGA and DSC curves of TN and TN-RxGy; CV data of TN and TN-RxGy; XRD patterns of TN-RxGy; EL characteristics of devices based on 0.03 mol % TN blended into PFB; ASE and emission characteristics of PF films; ¹H NMR, ¹³C NMR and MALDI-TOF mass spectra of TN and TN3Br; ¹H NMR of TN-RxGy (PDF)

AUTHOR INFORMATION

Corresponding Authors

*E-mail iamwylai@njupt.edu.cn (W.-Y.L.).

*Email: wei-huang@njtech.edu.cn (W.H.).

Author Contributions

C.-F.L. and Y.J. contributed equally to this work.

Notes

The authors declare no competing financial interest.

ACKNOWLEDGMENTS

The authors acknowledge financial support from the National Key Basic Research Program of China (973 Program, 2014CB648300), the National Natural Science Foundation of China (21422402, 20904024, 51173081, 61136003), the Natural Science Foundation of Jiangsu Province (BK20140060, BK20130037, BM2012010), Program for Jiangsu Specially-Appointed Professors (RK030STP15001), Program for New Century Excellent Talents in University (NCET-13-0872), Specialized Research Fund for the Doctoral Program of Higher Education (20133223110008, and 20113223110005), the Synergetic Innovation Center for Organic Electronics and Information Displays, the Priority Academic Program Development of Jiangsu Higher Education Institutions (PAPD), the NUPT "1311 Project", the Six Talent Plan (2012XCL035), the 333 Project (BRA2015374), and the Qing Lan Project of Jiangsu Province.

REFERENCES

- (1) D' Andrade, B. W.; Forrest, S. R. White Organic Light-emitting Devices for Solid-state Lighting. *Adv. Mater.* **2004**, *16*, 1585–1595.
- (2) Furuta, P. T.; Deng, L.; Garon, S.; Thompson, M. E.; Frechet, J. M. J. Platinum-functionalized Random Copolymers for Use in Solution-processible, Efficient, Near-white Organic Light-emitting Diodes. *J. Am. Chem. Soc.* **2004**, *126*, 15388–15389.
- (3) Huang, J.; Li, G.; Wu, E.; Xu, Q.; Yang, Y. Achieving High-Efficiency Polymer White-light-Emitting Devices. *Adv. Mater.* **2006**, *18*, 114–117.
- (4) Zou, J. H.; Liu, J.; Wu, H. B.; Peng, J. B.; Yang, W.; Cao, Y. High-efficiency and Good Color Quality White Light-emitting Devices Based on Polymer Blend. *Org. Electron.* **2009**, *10*, 843–848.
- (5) Chen, L.; Li, P. C.; Tong, K.; Xie, Z. Y.; Wang, L. Y.; Jing, X. B.; Wang, F. S. White Electroluminescent Single-polymer Achieved by Incorporating Three Polyfluorene Blue Arms into a Star-shaped Orange Core. *J. Polym. Sci., Part A: Polym. Chem.* **2012**, *50*, 2854–2862.
- (6) D'Andrade, B. W.; Brooks, J.; Adamovich, V.; Thompson, M. E.; Forrest, S. R. Controlling Exciton Diffusion in Multilayer White Phosphorescent Organic Light Emitting Devices. *Adv. Mater.* **2002**, *14*, 1032–1036.
- (7) Kim, J. H.; Herguth, P.; Kang, M. S.; Jen, A. K. Y.; Tseng, Y. H.; Shu, C. F. Bright White Light Electroluminescent Devices Based on a Dye-dispersed Polyfluorene Derivative. *Appl. Phys. Lett.* **2004**, *85*, 1116–1118.
- (8) Jou, J. H.; Sun, M. C.; Chou, H. H.; Li, C. H. Efficient Pure-white Organic Light-emitting Diodes with a Solution-processed, Binary-host Employing Single Emission Layer. *Appl. Phys. Lett.* **2006**, *88*, 141101.
- (9) Kim, T. H.; Lee, H. K.; Park, O. O.; Chin, B. D.; Lee, S. H.; Kim, J. K. White-light-emitting Diodes Based on Iridium Complexes via

Efficient Energy Transfer from a Conjugated Polymer. *Adv. Funct. Mater.* **2006**, *16*, 611–617.

(10) Granstrom, M.; Inganas, O. White Light Emission from a Polymer Blend Light Emitting Diode. *Appl. Phys. Lett.* **1996**, *68*, 147–149.

(11) Tasch, S.; List, E. J. W.; Ekstrom, O.; Graupner, W.; Leising, G.; Schlichting, P.; Rohr, U.; Geerts, Y.; Scherf, U.; Mullen, K. Efficient White Light-emitting Diodes Realized with New Processable Blends of Conjugated Polymers. *Appl. Phys. Lett.* **1997**, *71*, 2883–2885.

(12) Liu, J.; Zhou, Q. G.; Cheng, Y. X.; Geng, Y. H.; Wang, L. X.; Ma, D. G.; Jing, X. B.; Wang, F. S. The First Single Polymer with Simultaneous Blue, Green, and Red Emission for White Electroluminescence. *Adv. Mater.* **2005**, *17*, 2974–2978.

(13) Lee, S. K.; Jung, B. J.; Ahn, T.; Jung, Y. W.; Lee, J. I.; Kang, I. N.; Lee, J.; Park, J. H.; Shim, H. K. White Electroluminescence from a Single Polyfluorene Containing Bis-DCM Units. *J. Polym. Sci., Part A: Polym. Chem.* **2007**, *45*, 3380–3390.

(14) Tsami, A.; Yang, X. H.; Galbrecht, F.; Farrell, Tony.; Li, H. B.; Adamczyk, S.; Heiderhoff, R.; Balk, L. J.; Neher, D.; Holder, E. Random Fluorene Copolymers with On-chain Quinoxaline Acceptor Units. *J. Polym. Sci., Part A: Polym. Chem.* **2007**, *45*, 4773–4785.

(15) Shekhar, S.; Aharon, E.; Tian, N.; Galbrecht, F.; Scherf, U.; Holder, E.; Frey, G. L. Decoupling 2D Inter- and Intrachain Energy Transfer in Conjugated Polymers. *ChemPhysChem* **2009**, *10*, 576–581.

(16) Kanelidis, I.; Ren, Y.; Lesnyak, V.; Gasse, J. C.; Frahm, R.; Eychmueller, A.; Holder, E. Arylamino-Functionalized Fluorene- and Carbazole-Based Copolymers: Color-Tuning Their CdTe Nanocrystal Composites from Red to White. *J. Polym. Sci., Part A: Polym. Chem.* **2011**, *49*, 392–402.

(17) Lai, W. Y.; Zhu, R.; Fan, Q. L.; Hou, L. T.; Cao, Y.; Huang, W. Monodisperse Six-Armed Triazatruxenes: Microwave-Enhanced Synthesis and Highly Efficient Pure-Deep-Blue Electroluminescence. *Macromolecules* **2006**, *39*, 3707–3709.

(18) Lai, W.-Y.; He, Q. Y.; Zhu, R.; Chen, Q. Q.; Huang, W. Kinked Star-Shaped Fluorene/Triazatruxene Co-oligomer Hybrids with Enhanced Functional Properties for High-Performance, Solution-Processed, Blue Organic Light-Emitting Diodes. *Adv. Funct. Mater.* **2008**, *18*, 265–267.

(19) Xia, R. D.; Lai, W.-Y.; Levermore, P. A.; Huang, W.; Bradley, D. D. C. Low-Threshold Distributed-Feedback Lasers Based on Pyrene-Cored Starburst Molecules with 1,3,6,8-Attached Oligo(9,9-Dialkylfluorene) Arms. *Adv. Funct. Mater.* **2009**, *19*, 2844–2850.

(20) Lai, W.-Y.; Xia, R. D.; He, Q. Y.; Levermore, P. A.; Huang, W.; Bradley, D. D. C. Enhanced Solid-State Luminescence and Low-Threshold Lasing from Starburst Macromolecular Materials. *Adv. Mater.* **2009**, *21*, 355–360.

(21) Lai, W.-Y.; Chen, Q. Q.; He, Q. Y.; Fan, Q. L.; Huang, W. Microwave-enhanced Multiple Suzuki Couplings toward Highly Luminescent Starburst Monodisperse Macromolecules. *Chem. Commun.* **2006**, *18*, 1959–1961.

(22) Lai, W.-Y.; Xia, R.; Bradley, D. D. C.; Huang, W. 2,3,7,8,12,13-Hexaaryltruxenes: an Ortho-substituted Multiarm Design and Microwave-accelerated Synthesis toward Starburst Macromolecular Materials with Well-defined pi Delocalization. *Chem. - Eur. J.* **2010**, *16*, 8471–8479.

(23) Zhao, L. L.; Jiu, Y. D.; Wang, J. Y.; Zhang, X. W.; Lai, W.-Y.; Huang, W. Synthesis and Characterization of Starburst Conjugated Molecules with Multiple p-n Branches for Narrow Band Gap Modulation. *Acta Chim. Sinica* **2013**, *71*, 1248–1256.

(24) Sun, M. H.; Fu, Y. Q.; Li, J.; Bo, Z. S. Star Polyfluorenes with a Triphenylamine-Based Core. *Macromol. Rapid Commun.* **2005**, *26*, 1064–1069.

(25) Li, B.; Xu, X. J.; Sun, M. H.; Fu, Y. Q.; Yu, G.; Liu, Y. Q.; Bo, Z. S. Porphyrin-Cored Star Polymers as Efficient Nondoped Red Light-Emitting Materials. *Macromolecules* **2006**, *39*, 456–461.

(26) Liu, J.; Cheng, Y. X.; Xie, Z. Y.; Geng, Y. H.; Wang, L. X.; Jing, X. B.; Wang, F. S. White Electroluminescence from a Star-like Polymer with an Orange Emissive Core and Four Blue Emissive Arms. *Adv. Mater.* **2008**, *20*, 1357–1363.

(27) Chen, L.; Li, P. C.; Cheng, Y. X.; Xie, Z. Y.; Wang, L. X.; Jing, X. B.; Wang, F. S. White Electroluminescence from Star-like Single Polymer Systems: 2,1,3-Benzothiadiazole Derivatives Dopant as Orange Cores and Polyfluorene Host as Six Blue Arms. *Adv. Mater.* **2011**, *23*, 2986–2990.

(28) He, R. F.; Xu, J.; Xue, Y.; Chen, D. C.; Ying, L.; Yang, W.; Cao, Y. Improving the Efficiency and Spectral Stability of White-emitting Polycarbazoles by Introducing a Dibenzothiophene-S,S-dioxide Unit into the Backbone. *J. Mater. Chem. C* **2014**, *2*, 7881–7890.

(29) Jiu, Y. D.; Liu, C. F.; Wang, J. Y.; Lai, W.-Y.; Jiang, Y.; Xu, W. D.; Zhang, X. W.; Huang, W. Saturated and stabilized white electroluminescence with simultaneous three color emission from a six-armed star-shaped single-polymer system. *Polym. Chem.* **2015**, *6*, 8019–8028.

(30) Kim, J.; Park, J.; Jin, S. H.; Lee, T. S. Synthesis of conjugated, hyperbranched copolymers for tunable multicolor emissions in light-emitting diodes. *Polym. Chem.* **2015**, *6*, 5062–5069.

(31) McGehee, M. D.; Heeger, A. J. Semiconducting (Conjugated) Polymers as Materials for Solid-State Lasers. *Adv. Mater.* **2000**, *12*, 1655–1668.

(32) Yap, B. K.; Xia, R.; Campoy-Quiles, M.; Stavrinou, P. N.; Bradley, D. D. C. Simultaneous Optimization of Charge-carrier Mobility and Optical Gain in Semiconducting Polymer Films. *Nat. Mater.* **2008**, *7*, 376–380.

(33) Yu, L.; Liu, J.; Hu, S.; He, R.; Yang, W.; Wu, H.; Peng, J.; Xia, R.; Bradley, D. D. C. Red, Green, and Blue Light-Emitting Polyfluorenes Containing a Dibenzothiophene-S,S-Dioxide Unit and Efficient High-Color-Rendering-Index White-Light-Emitting Diodes Made Therefrom. *Adv. Funct. Mater.* **2013**, *23*, 4366–4376.

(34) Xu, W.; Yi, J.; Lai, W.-Y.; Zhao, L.; Zhang, Q.; Hu, W.; Zhang, X.-W.; Jiang, Y.; Liu, L.; Huang, W. Pyrene-Capped Conjugated Amorphous Starbursts: Synthesis, Characterization, and Stable Lasing Properties in Ambient Atmosphere. *Adv. Funct. Mater.* **2015**, *25*, 4617–4625.

(35) Xia, R.; Heliotis, G.; Campoy-Quiles, M.; Stavrinou, P. N.; Bradley, D. D. C.; Vak, D.; Kim, D. Y. Characterization of a High-thermal-stability Spiroanthracene-fluorene-based Blue-light-emitting Polymer Optical Gain Medium. *J. Appl. Phys.* **2005**, *98*, 083101–083106.